

## General Disclaimer

### One or more of the Following Statements may affect this Document

- This document has been reproduced from the best copy furnished by the organizational source. It is being released in the interest of making available as much information as possible.
- This document may contain data, which exceeds the sheet parameters. It was furnished in this condition by the organizational source and is the best copy available.
- This document may contain tone-on-tone or color graphs, charts and/or pictures, which have been reproduced in black and white.
- This document is paginated as submitted by the original source.
- Portions of this document are not fully legible due to the historical nature of some of the material. However, it is the best reproduction available from the original submission.

UNITED STATES  
DEPARTMENT OF THE INTERIOR  
GEOLOGICAL SURVEY

INTERAGENCY REPORT NASA-146

PREDICTING THE RELATIVE DYE LAYER DENSITIES  
OF COLOR INFRARED TRANSPARENCIES

by

Robert W. Pease  
Department of Geography  
University of California  
Riverside, California

January 1969

FACILITY FORM 602	N71-34361	
	(ACCESSION NUMBER)	
	36	(THRU)
	(PAGES)	63
	CR-121658	(CODE)
	(NASA CR OR TMX OR AD NUMBER)	14
		(CATEGORY)



Prepared by the Geological Survey for the National Aeronautics and Space Administration (NASA) under Contract No. R-09-020-024(A/1), Task No. 160-75-01-32-10. Work performed under USGS/Geographic Applications Program Contract No. 14-08-0001-10674 with the University of California

## ABSTRACT

A graphical method is presented whereby relative dye-layer densities of color infrared image elements can be derived from known reflectance curves. The response of each dye-forming layer in 50 nanometer wavebands across the CIR spectrum are totaled and plotted on a  $D \log E$  diagram for type 8443 film, a diagram modified to fit an illumination with constant intensity for all wavelengths. From the relative dye-layer densities so derived, hue and tone of image elements can be inferred.

Application of the method is made for some common image targets showing (1) how plant reflection yields a red record, (2) the unbalancing effect of air luminance on the color of the image, (3) the reshaping of the spectral distribution of energy reaching the film with auxiliary filters to overcome this imbalance, and (4) the nature of the record for certain targets other than vegetation both at close range and aloft.

In addition an analysis is made using the method to show the effect of spectral characteristics of certain spacecraft windows on possible CIR photography through them. Space-deteriorated coatings will not yield a satisfactory CIR image whereas non-deteriorated or uncoated windows will do so.

## FOREWORD

The use of color infrared film (Kodak Ektachrome Infrared Aero, Type 8443) as a spacecraft sensor faces certain obstacles when used to photograph through present space ports. One obstacle is the necessity for overcoming the color imbalance that results from air luminance and another is the effect spacecraft window coatings will have on the red infrared record. Although the graphical method for predicting the possible success of the film as a spacecraft remote sensor outlined harkens back to a pre-computer era, it gives a ready means for assessing results that will be obtained and possible auxiliary filters that should be used. The report also provides conceptual information for the non-professional photographer user of this unique source of remotely sensed information.

We would like to thank Norman Fritz of Eastman Kodak Company for his suggestions relating to this report which have been incorporated in it.

Leonard W. Bowden  
Principal Investigator  
Southern California Test Site 130

Robert W. Pease  
Investigator

## PREDICTING THE RELATIVE DYE LAYER DENSITIES OF COLOR INFRARED TRANSPARENCIES

Occasions arise when it is desirable to predict in advance the probable success of color infrared film to yield a meaningful red record. Whether or not to use the film or the intelligent choice of appropriate minus-visual auxiliary filters to combat the effects of altitude (Pease and Bowden, 1968) will save time and funds when planning a CIR photo mission.

The need for prediction arises from the fact that the infrared-recording or cyan-forming layer in the film has been designed with less sensitivity than either of the other two layers. Thus exposure spectrally available to this layer must be significantly greater than that of either of the other layers in order that cyan density in the finished transparency be the lowest of the three, a condition necessary for a red balance. This need is in contradiction to daylight as an illuminant for the major sensitivity of the cyan-forming layer is to the weakest part of the sunlight energy distribution in the CIR waveband, 500-900 nanometers.

In making an assessment of relative dye-layer densities, it is necessary to know the spectral distribution of energy reaching the film. By a graphical method later described, this can be plotted on a modified D Log E diagram for the film (Kodak Ektachrome Infrared Aero, Type 8443) to determine densities. Energy reaching the film will be the energy reaching the camera, attenuated by the combined transmittances of all filters used with the CIR system. When photos are to be taken through spacecraft windows, the transmittance characteristics of the window and its coatings must be considered as another attenuating filter.

The energy reaching a high altitude photo platform will have a spectral distribution that will consist of the reflection from the ground target, attenuated somewhat in the near infrared by water vapor in the light path, to which has been added the energy of air luminance from the atmospheric upscatter of sunlight. The reflection or energy leaving the target will have a spectral distribution that is the sunlight illumination molded by the reflectance of the target materials. Reflectance is a property of the target that is independent of the nature of the illumination (Fig. 1).

#### THE METHOD

A graphical method has been used in making density determinations. This involves (1) plotting the spectral curve of energy reaching the film, (2) weighting the energy available in discrete wavebands with an effectiveness factor for the sensitivity in the band of each dye-layer, and (3) plotting the summations of exposure for each dye layer on a  $D \log E$  sensitometric diagram for Type 8443 film, modified for this method of analysis.

Basic details of the procedure are illustrated with the aid of the following graphical representations. With one exception, reflection curves were actually measured in nature at Southern California sites with the aid of an ISCO Model SR spectroradiometer.

#### Some Sensitometric Considerations

Since placement of the sensitometric curve of the cyan layer with respect to the curves of the other layers is critical to the relative positions of the dye-layer densities, it was found necessary to modify a  $D \log E$  diagram to fit this method of graphical analysis. The sensitometric diagrams presented by Fritz (1967) and Tarkington and Sorem (1963) appear to use daylight as

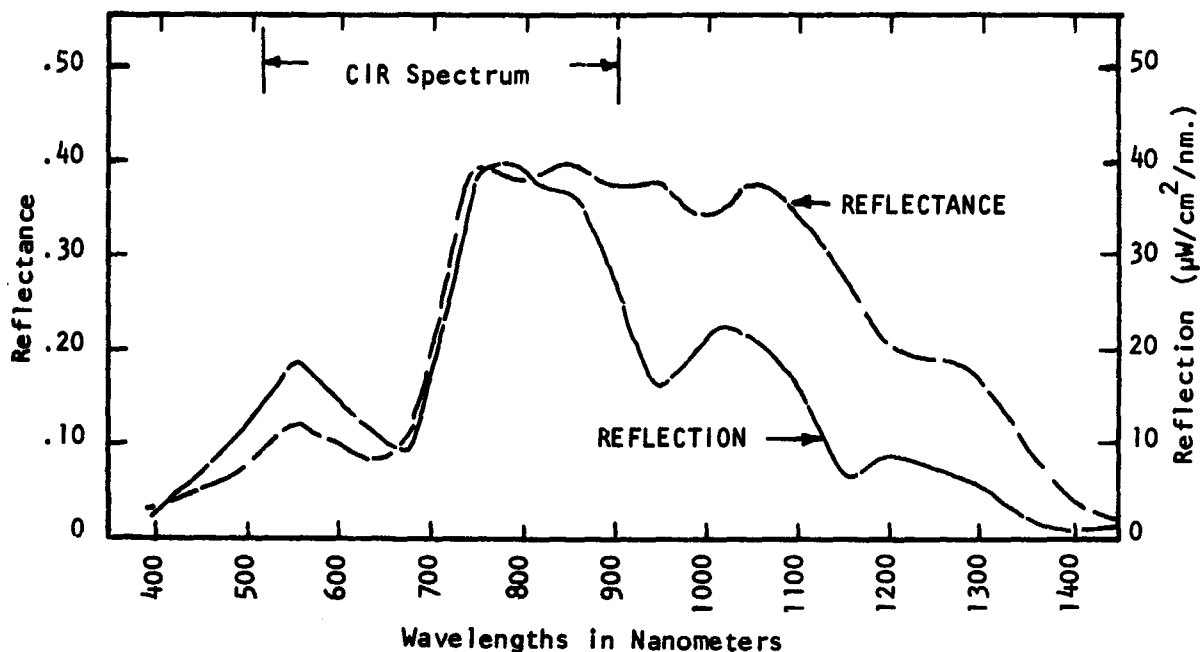


Fig. 1. Reflection vs. reflectance. Reflectance is a property of a target that is independent of the spectral distribution of illumination. For any wavelength, it is the fraction of the incident energy that will be reflected. In this manner reflectance molds the spectral curve of illumination into the curve of reflection or energy that leaves the target.

This figure shows curves of reflectance and reflection superimposed in such a way that values coincide at 750 nm. It is to be noted that the sunlight peak near 550 nm. causes reflection to be higher in the visual, but to drop off or be lower in the near infrared.

For a specific target, the curve of energy reflected will vary with the nature of the illumination according to atmospheric conditions and the altitude of the sun. A typical solar curve, measured in Riverside, California, is used for the following illustrative graphs (Fig. 5).

illumination. In the method here presented, however, the infrared decline of daylight is taken into account in the curves from which exposure values are derived and the placement of the cyan sensitometric curve is that which would be appropriate for a hypothetical illumination that unlike daylight would have constant intensity across the spectrum. This strengthens the infrared energies and moves the cyan curve closer on the D log E diagram to the curves of the other layers.

The following method was used to determine the degree of displacement of the cyan curve. A neutral target<sup>1</sup> was illuminated with a 3400°K light. Appropriate filters were used with the film to render the target close to neutral (actually varied from cyan-gray at low density to gray-green at high density). The spectral distribution of light reaching film was measured with an ISCO spectroradiometer and the D log E curves placed to properly render both low and high density color balances. With this placement, the cyan layer requires close to twice the exposure of the other layers to achieve the same density.

The curve placements should be such that the relative layer densities derived from a known set of conditions approach reality. In practice it has been noted that when an 80B filter is auxiliary to the minus-blue, weathered soil targets are rendered aloft close to neutral. To test the modified D log E diagram, a graphical analysis was made of this condition (Fig. 13) and the relative densities rather accurately described the color achieved. Pine needles and neutral targets aloft are represented closely by figures 9 and 12, respectively. It is felt, therefore, that this placement of the cyan

---

<sup>1</sup>An 18 percent Kodak neutral gray card with a Wratten 15 as the minus-blue filter. See Appendix.



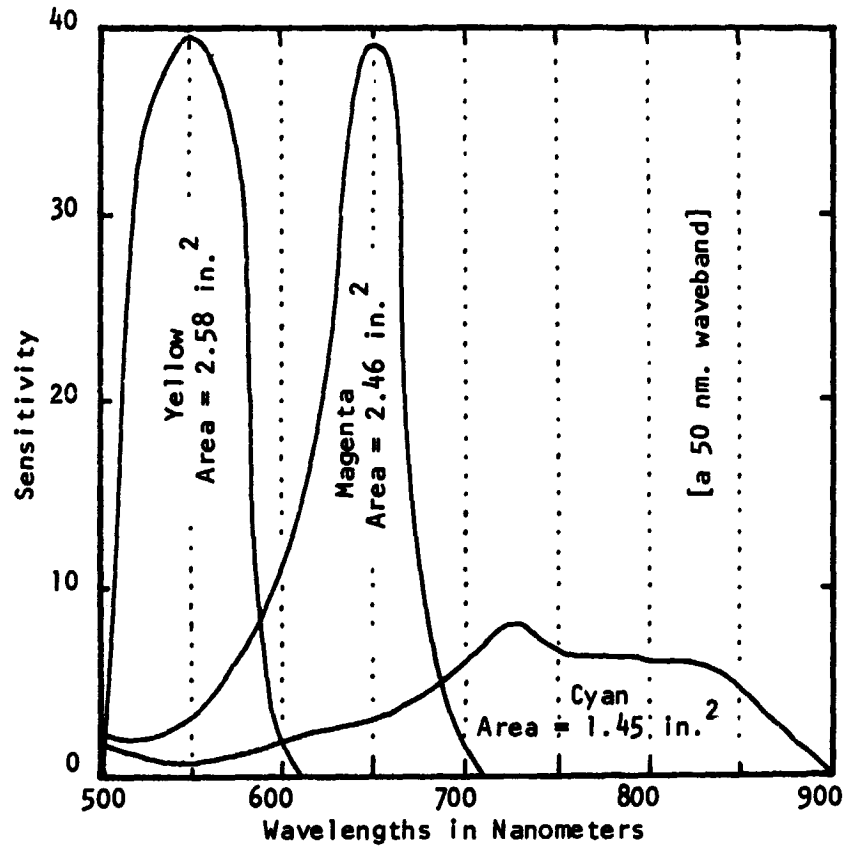


Figure 2. Linear plots of the film layer sensitivities of Type 8443 CIR film using a minus-blue filter. The curves have been constructed from the logarithmic plots of Fritz (1967). The fraction of each dye-layer exposure occurring in each 50 nm. waveband is as follows.

<u>nm.</u>	<u>Yellow</u>	<u>Magenta</u>	<u>Cyan</u>
500-550	.52	.04	.01
550-600	.48	.13	.03
600-650		.50	.08
650-700		.33	.14
700-750			.25
750-800			.21
800-850			.20
850-900			.08

sensitometric curve is most useful for the graphical analysis of relative dye-layer densities here described.

Sensitometrically, the three dye-layers do not occupy discrete spectral bands. There is some overlap between the yellow- and magenta-forming layers and the cyan-forming layer extends with varying sensitivity across the whole CIR spectrum. To realize a rational exposure for any layer, its entire range of sensitivity must be taken into consideration. To accomplish this, the linear plot of the spectral sensitivity diagram (Fig. 2) was divided into the 50 nm. wavebands. The fraction of the total exposure of a layer falling into a band provides a weighting factor to be applied against that portion of the energy curve reaching the film that falls into the band. This is demonstrated for pine needles on a sample worksheet (Fig. 4). The summation of the weighted waveband areas for any dye-forming layer constitutes the exposure of that layer.

Although exposure is expressed as a logarithmic value, a linear scale is included for exposure on the following graphs. Logs of the exposures can be plotted on a linear scale with perhaps greater accuracy than when placing exposure directly onto a logarithmic grid.

Figure 3 plots densities for pine needles as a close-range plant target. Figure 4 shows the worksheet that is used to weigh exposure effectiveness in each of the 50 nm. bands. These two figures illustrate the method employed.

#### A Sample Plotting

Curve A in the lower graph of Figure 3 is the reflection from pine needles measured directly in energy terms with an ISCO spectroradiometer. A similar curve could have been constructed by integrating the reflectance curve for the pine needles with an appropriate sunlight illumination curve.

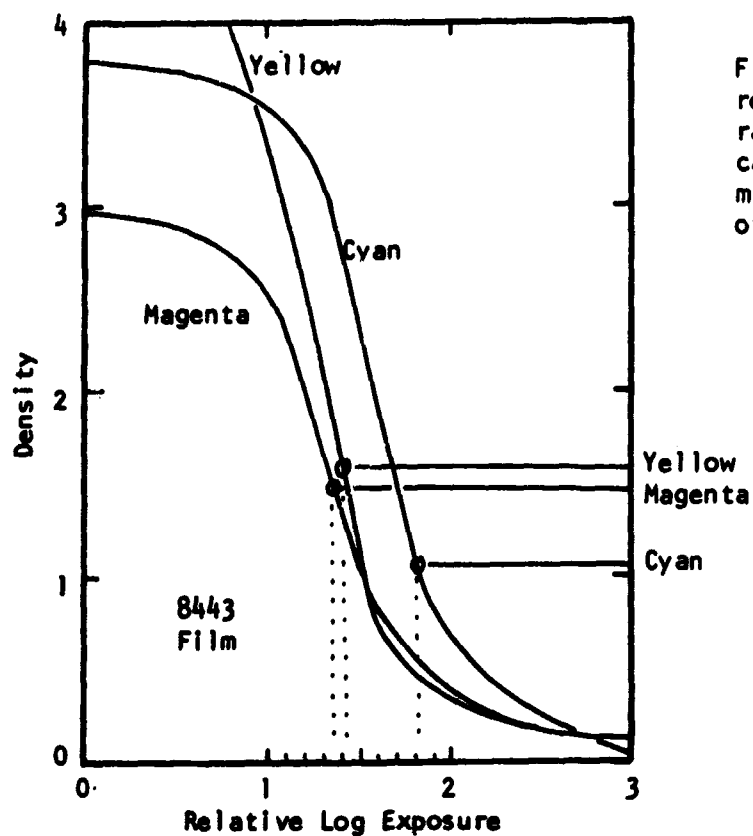
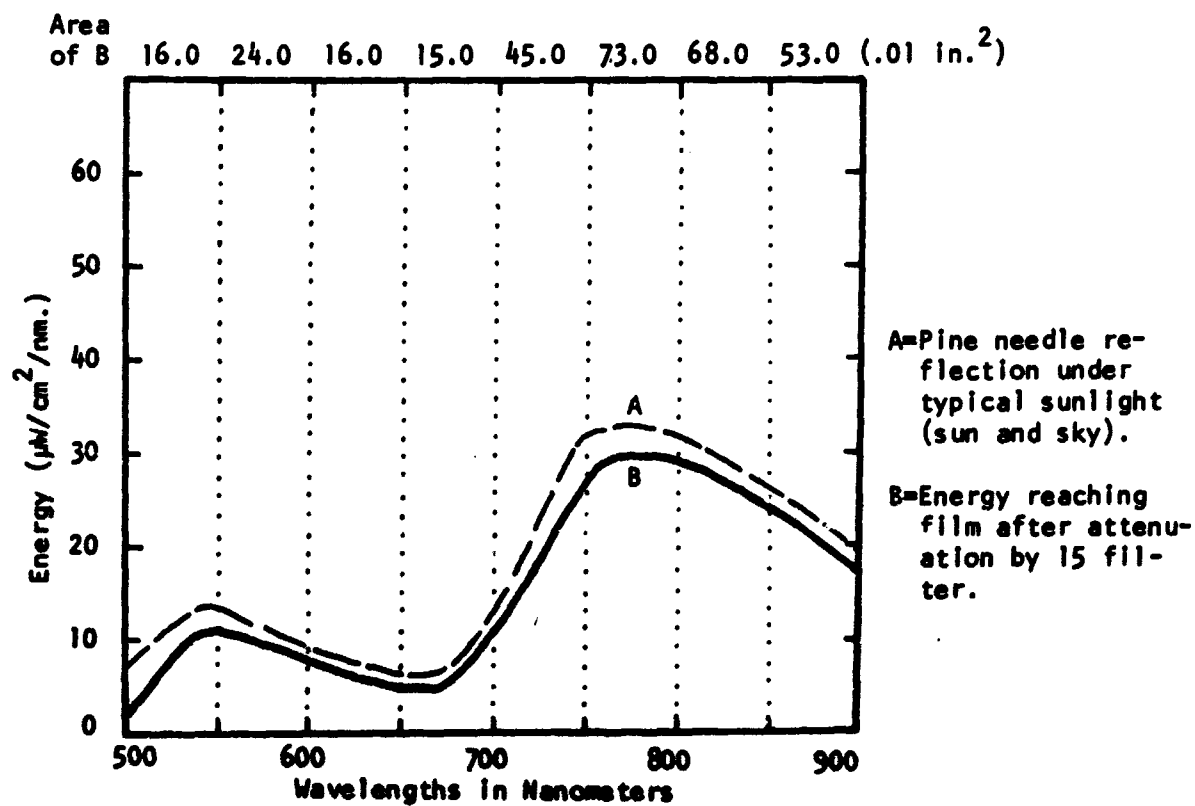


Figure 3. Pine needle reflection at close range, attenuated at camera only by the minus-blue (15) filter of the CIR system.



Target PINE NEEDLES - CLOSEFilters 15 ONLY

EXPOSURE EFFECTIVENESS OF FILM LAYERS FOR 50 NM SPECTRAL WAVEBANDS  
(Expressed as fractions of total exposure of film layer)

Zone boundary	Area in zone	Weighting factors and band exposures					
		<u>Yellow</u>		<u>Magenta</u>		<u>Cyan</u>	
500	16.0	.52	8.35	.04	0.64	.01	0.16
550	24.0	.48	11.50	.13	3.14	.03	0.72
600	16.0			.50	8.00	.08	1.28
650	15.0			.33	4.95	.14	2.10
700	45.0					.25	11.30
750	73.0					.21	14.80
800	68.0					.20	13.60
850	53.0					.08	4.30
900							
Totals			<u>19.85</u>		<u>16.73</u>		<u>48.26</u>

	<u>Weighted areas</u>	<u>x</u>	<u>Exposure</u>	<u>Log Exposure</u>
Yellow	19.85	1.3	25.60	1.41
Magenta	16.73	1.3	21.70	1.34
Cyan	48.26	1.3	63.00	1.80

"x" is a factor of convenience to place the exposure on the straight line segment of the curves. It is dimensionless, but roughly correlates with camera exposure manipulation

Figure 4. A sample worksheet and calculations. For the curve of energy reaching the film, the area in each of the 50 nm. wavebands is appropriately weighted for each layer (Fig. 2). Summations for each film layer are entered on the  $\log E$  diagrams as logs of the exposures. These calculations were used to make Fig. 3.

Curve A is the energy reaching the camera. Curve B plots the energy after it has been attenuated by a Wratten 15 filter, a basic minus-blue filter for the CIR system.<sup>2</sup> This is the energy actually reaching the film.

The area within Curve B in each of the 50 nm wavebands is then measured. The number at the top of the column is the number of .01 in<sup>2</sup> squares within the curve in the 50 nm. band. These areas are proportional to the energy available to the film in each band. A 50 nm. band appears to be a good compromise that permits speed in computation and a desirable order of accuracy.

The waveband areas are entered on a worksheet (Fig. 4) where they are used as functions with the exposure effectiveness weighting factors the sheet provides to calculate the effective exposure of each film layer in each band. The summations of the effective exposure for each layer is then multiplied by a factor (X) that will cause the D log E plottings to fall on the straight-line portions of the curves. In general, a factor that places the cyan exposure between 50 and 90 will give a good result. Of course, the same factor must be applied to summations for each of the layers. Logarithms of the exposures are ascertained and density points are plotted on the D log E diagram.

In the pine needle example, the cyan layer density is moderately lower than those of the other layers. This is compatible with experience with CIR photos of this target using only minus-blue filtration. A moderate lowering of the IR/Visual reflectance ratio of a coniferous target causes cyan to predominate and the red record to be lost. This has made the CIR system useful in studying vigor and disease in coniferous forests. For a target with a higher IR/Visual reflectance ratio, such as broadleaf forest in new foliage or grass, the cyan density would be lower.

---

<sup>2</sup> A Wratten 15 has been used as the basic minus-blue filter in these graphs. Eastman Kodak Company recommends a 12 which lowers yellow density slightly.

## HIGH ALTITUDE USE

Although the pine needle target will yield a red record at close range it will not do so with the conventional CIR system at high altitudes. Deterioration of the red results from (1) a moderate amount of absorption of the near-infrared wavelengths by water vapor, particularly near 750 and 900 nanometers, and (2) the unbalancing spectrally of exposure that results from the addition of energy by the upscatter of light of air luminance.

### Air Luminance

Upscatter is spectrally selective according to the ratio of Rayleigh ( $\lambda^{-4}$ ) to Mie ( $\lambda^0$ ) scattering that is taking place. Rarely is air so pure that a  $\lambda^{-4}$  upscatter of energy exists (Brock et al, 1965). Conversely, all upscatter must include a component of Rayleigh scattering so that a  $\lambda^0$  luminance would be similarly impossible. A wide variety of upscatter spectral curves between these two extremes can thus exist. When haze is heavy the amount of upscatter will be high and will approach a Mie curve. If haze is very light this contribution to overall exposure will be small and will approach a Rayleigh spectral distribution. Harvey and Myskowski (in Brock, et al, 1965) suggest that an  $\lambda^{-1}$  to  $\lambda^{-2}$  are probably most typical. With one exception, the following graphs use a  $\lambda^{-2}$  upscatter which represents a condition with little haze (Fig. 5).

The amplitude of the upscatter bears an important relationship to the exposure balance of the film. Experimental observation with a broadband spectroradiometer that measures in both the visual and near infrared spectral realms suggests that a  $\lambda^{-2}$  very light haze condition returns approximately 8 percent of the incident illumination toward space. This is in agreement with observed values given in Brock (1965) for upscatter in the spectral band of

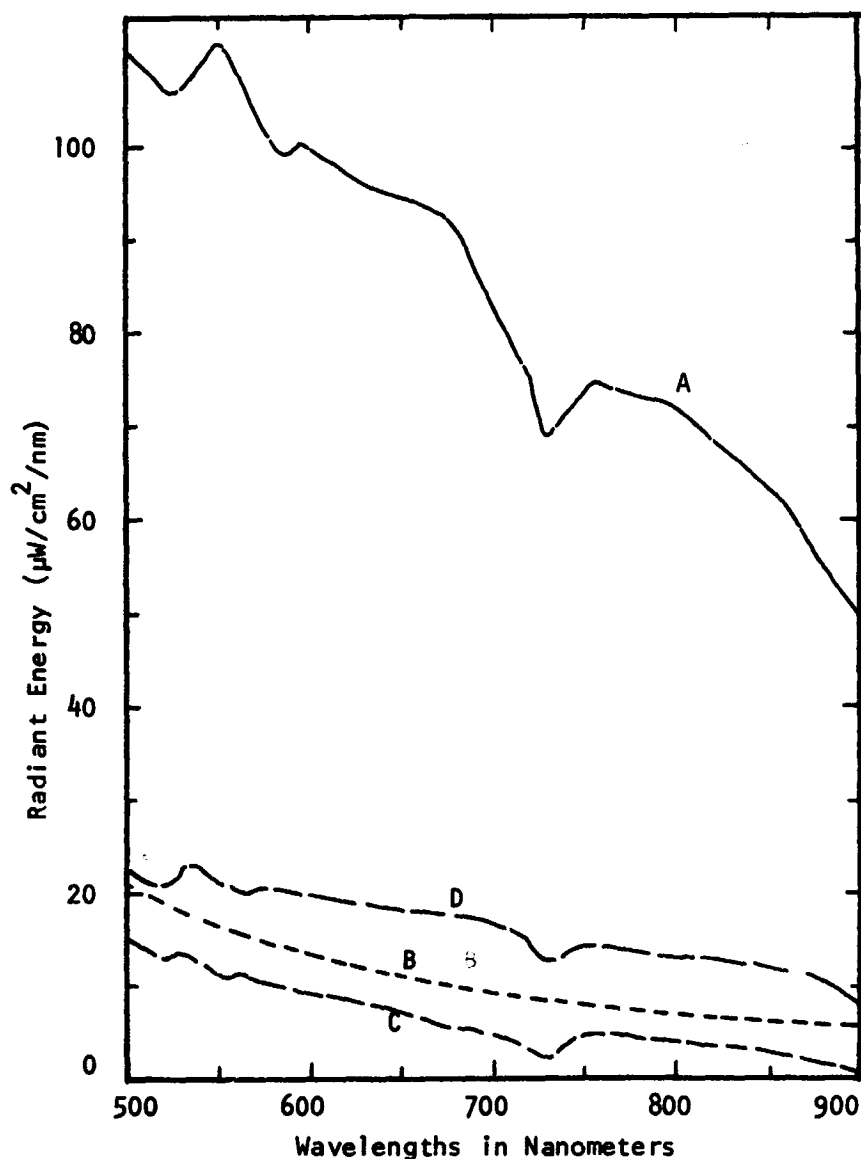


Figure 5. Upscatter of energy to high altitudes from air luminance. Upscatter of energy that will be added to the target reflection will be a portion of the incident solar illumination, modified according to the size of the molecules or particles doing the scattering. A typical solar curve (A) declines markedly toward the longer wavelengths. The dip at 750 nm. is due to water vapor absorption and will thus be present in the upscatter distribution. Curve B is a theoretical  $\lambda^{-2}$  distribution for a spectrally uniform illumination. It is included for comparison. Curve C is a  $.08 \lambda^{-2}$  upscatter of curve A and thus drops more sharply toward the longer wavelengths than the theoretical curve B. Curve D is a  $.20\lambda^0$  (Mie) distribution that also declines due to the solar curve it scatters.

540-720 nm. In all likelihood  $\lambda^{-4}$  or pure Rayleigh scattering would be in the order of 5 to 6 percent, while luminance approaching a Mie condition would return 20 percent or more. Except for the example showing the unbalancing effect of pure Mie upscatter, a .08 return with a  $\lambda^{-2}$  distribution is used in the following graphs as being a typical mild luminance condition.

#### The Effect of Upscatter on Exposure Balance

Although a decrease in infrared exposure by water vapor absorption in the optical path is a factor working against a red infrared record at high altitudes, the additional exposure of air luminance can well be of greater importance. In Figure 6, the addition of a .08  $\lambda^{-2}$  upscatter to the pine needle reflection places the cyan density on the D log E diagram above those of the other layers. The result will be a low color saturation, blue-green record for this target which records as red at close range. The upscatter added is that which would occur on a relatively clear day with little haze in the air. Only when the ratio of infrared to visual reflection strongly favors the infrared can a red record be obtained at high altitudes with the filtration recommended by the manufacturer of the film. Grass according to Fritz (1967) has close to an 8:1 IR/Visual reflectance ratio, which when plotted (Fig. 7) gives a cyan density well below that of the magenta layer.

The fact that  $\lambda^{-2}$  upscatter adds more energy to the shortwave end of the CIR exposure spectrum than to the long wave end causes it to have a marked effect in changing the spectral exposure balance. However, a pure Mie ( $\lambda^0$ ) upscatter, if such were theoretically possible, would be similarly effective. The .20  $\lambda^0$  upscatter of energy added to the pine needle reflection in Figure 8, by building up exposure energy in all wavelengths, reduces the spectral contrast in a manner similar to the reduction of scene contrasts by



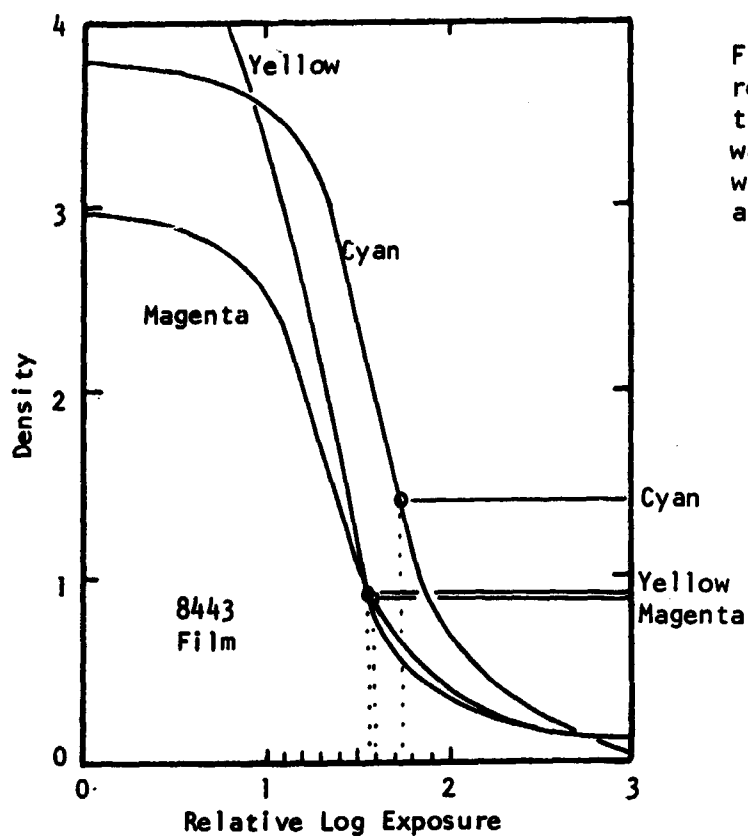
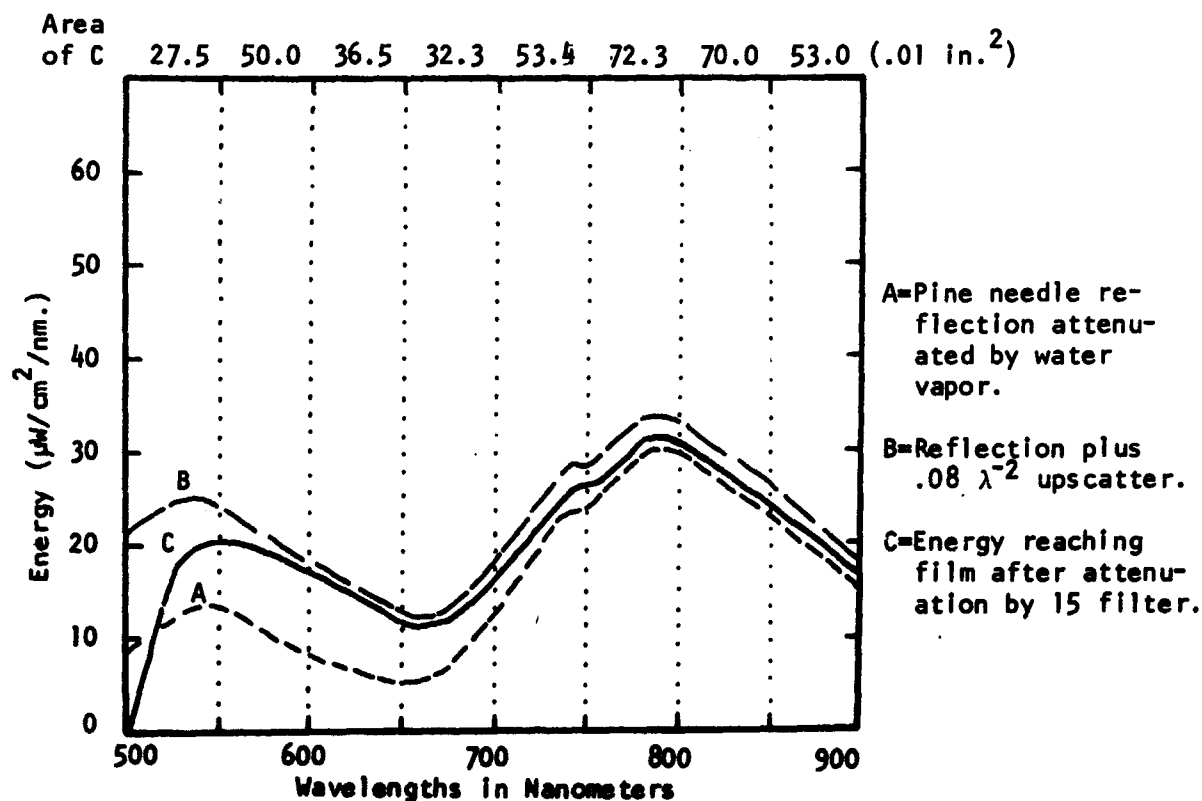


Figure 6. Pine needle reflection at high altitude, attenuated by water vapor at 750 nm, with  $.08\lambda^{-2}$  upscatter added to the exposure.



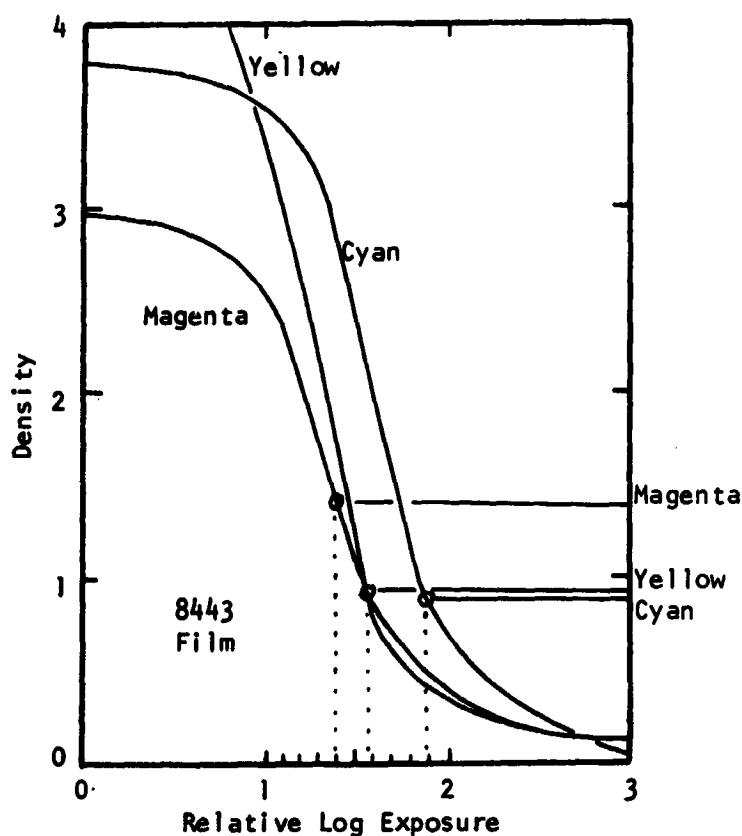
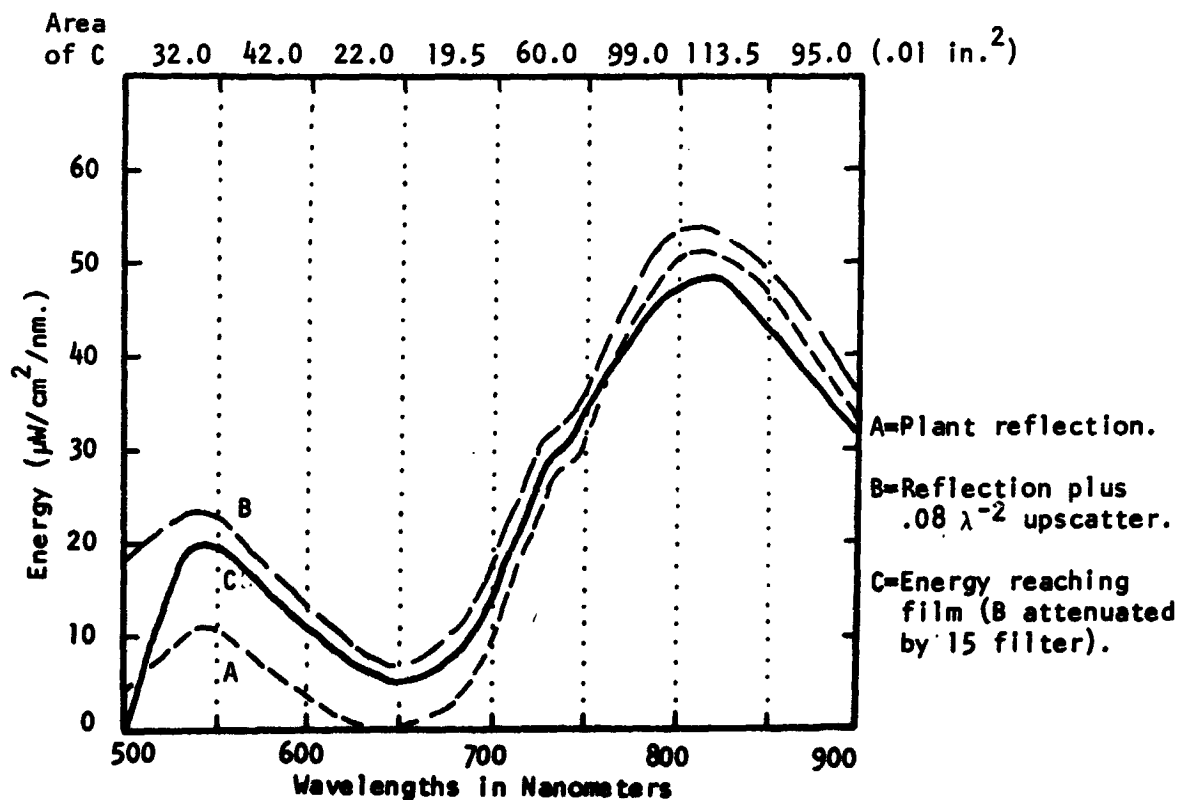


Figure 7. A high IR re-  
flectance target (grass)  
at high altitude. For  
this target red would  
show with only a 15 fil-  
ter despite moderate up-  
scatter from luminance.



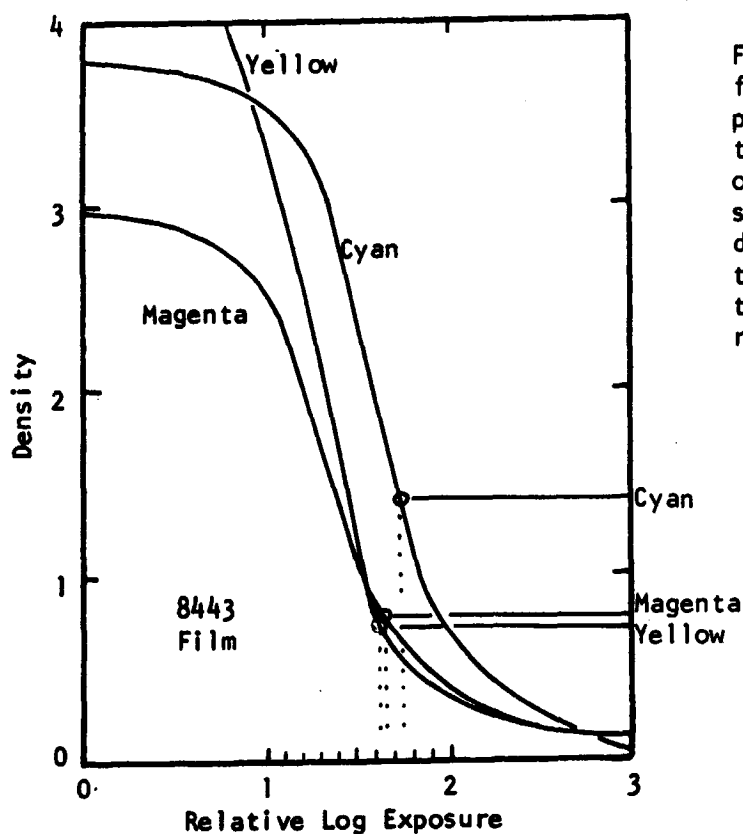
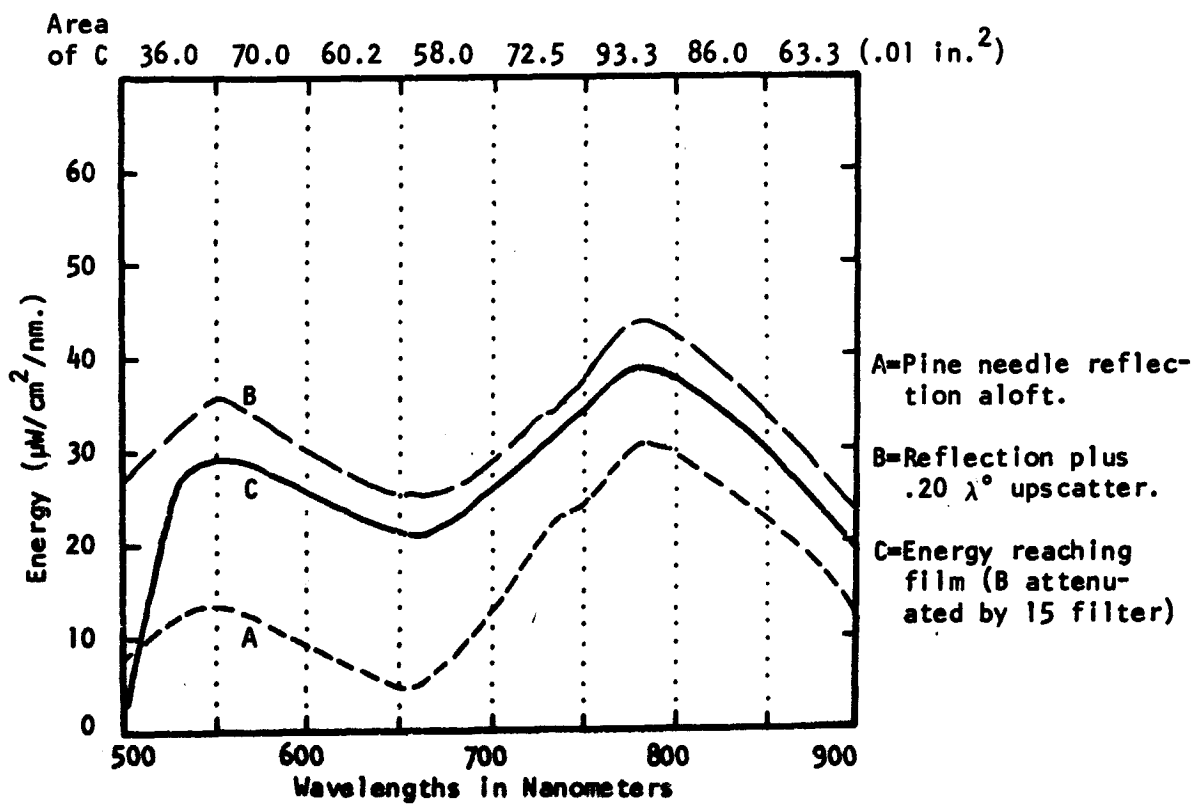


Figure 8. Pine needle reflection at high altitude plus a  $.20 \lambda^\circ$  (Mie) upscatter. Although the upscatter of light is close to being spectrally neutral, the addition of this energy to the target reflection changes the visual-infrared balance reaching the camera.



air luminance. As is illustrated, this will reduce the IR/Visual exposure ratio and cyan density will predominate. It should be noted that a  $\lambda^0$  curve will decline at its longwave end when it upscatters sunlight.

#### The Use of Minus-Visual Filters

The effects on exposure balance wrought by water vapor attenuation and the addition of air luminance or upscatter can be offset by the use of filters that attenuate the visual wavebands but not the near infrared. Several dye filters which essentially do this have been described by Pease and Bowden (1968). When these are used as auxiliaries to the basic minus-blue filter, spectral transmittance characteristics remold by selective attenuation the energy curve reaching the camera. Curve B in the spectral energy plot of Figure 9 indicates the energy reaching the film after it has been attenuated by the 15 and an 80B filters. Attenuation in the visual band is sufficiently strong that again the relative infrared exposure will yield a cyan density lower than the yellow or magenta. In fact the cyan is lower than is the case with a 15 filter alone at close range.

Not all components of the image are vegetation targets, however. Many urban targets, for example, are close to neutral, with a nearly equal reflectance to all wavelengths of the CIR spectrum. Figure 10 plots a .15 reflectance neutral target photographed at close range. Cyan predominates. Even though the target has a constant reflectance, there is a measure of decline toward the IR end due to the solar illumination curve it reflects. When the neutral target reflection is remolded by an 80B filter (Fig. 11) the balance is closer to neutral, but when upscatter is added (Fig. 12) cyan again predominates but with magenta relatively dense. The result is a bluish hue which experience has shown to be characteristic for urban targets when an 80B filter is used.

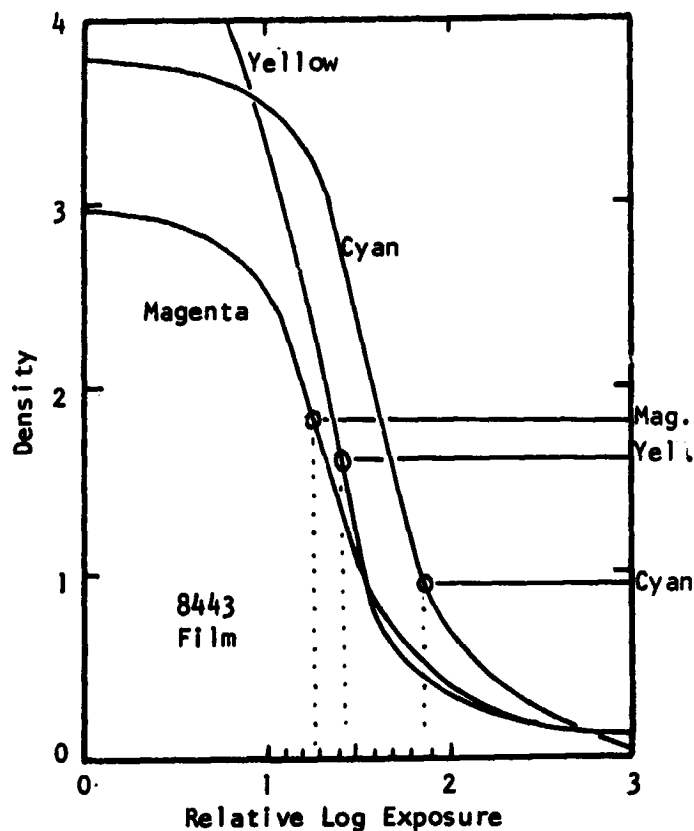
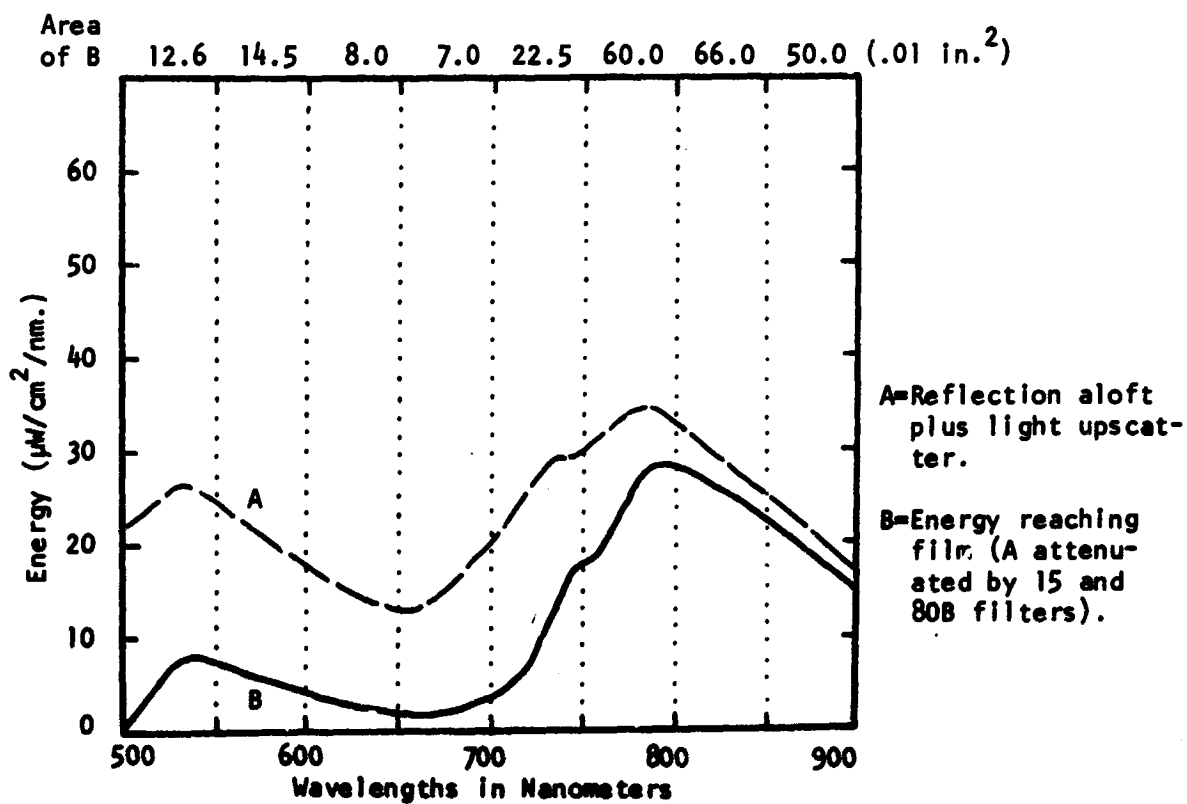


Figure 9. Pine needle reflection at high altitude with a minus-visual (80B) auxiliary filter. Light upscatter is  $.08 \lambda^{-2}$ . By remolding the spectral distribution of energy reaching the film with the 80B filter, the cyan density is rendered far lower than the densities of the other dye layers.

Auxiliary filters must fit Wratten specifications in the near-infrared



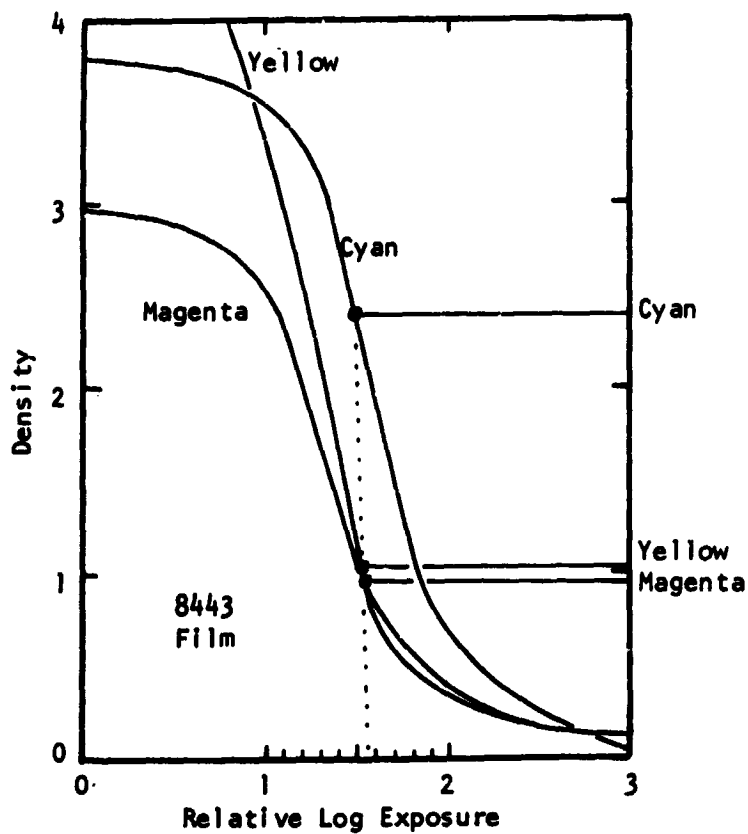
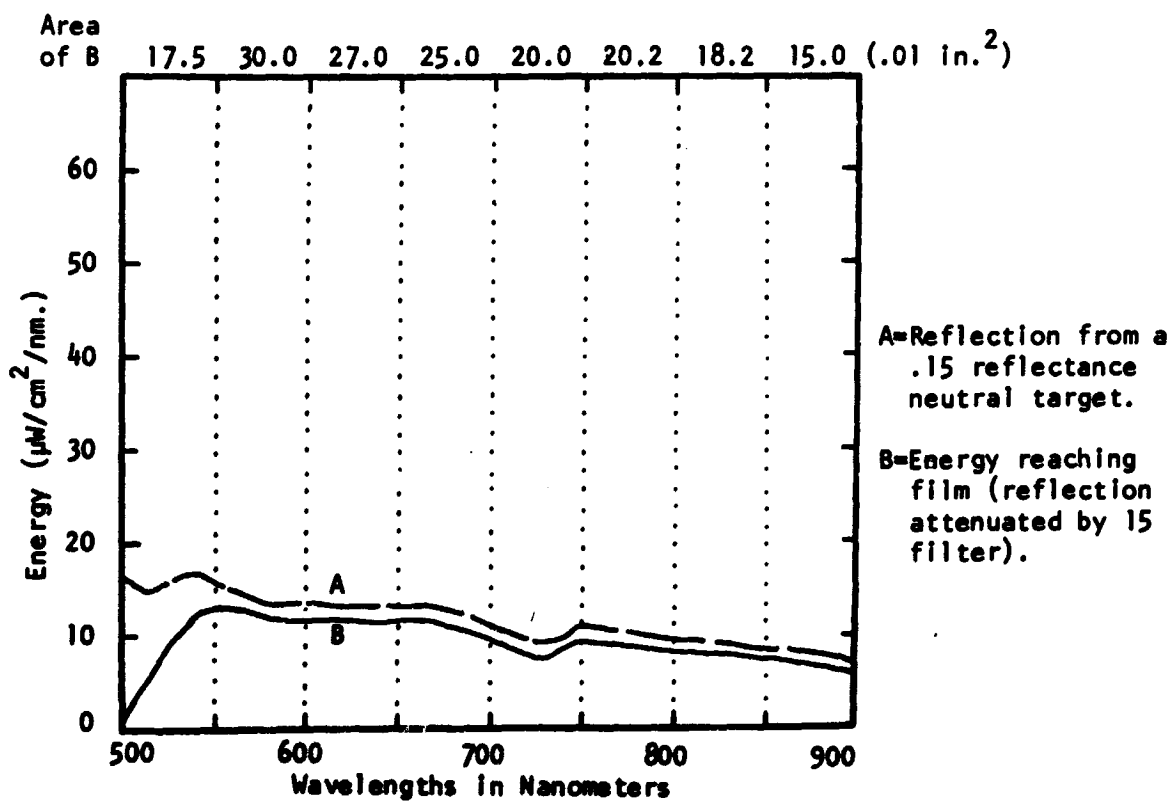


Figure 10. Reflection from a neutral target illuminated by the daylight shown in Fig. 5. When using only a minus-blue filter with a neutral target, cyan must predominate due to the lower sensitivity of the layer.



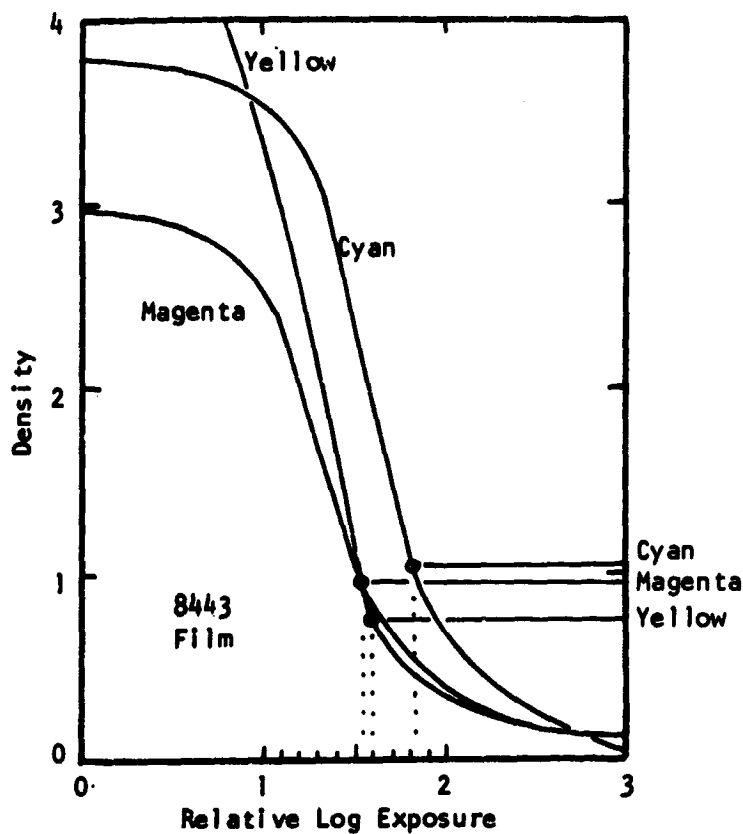
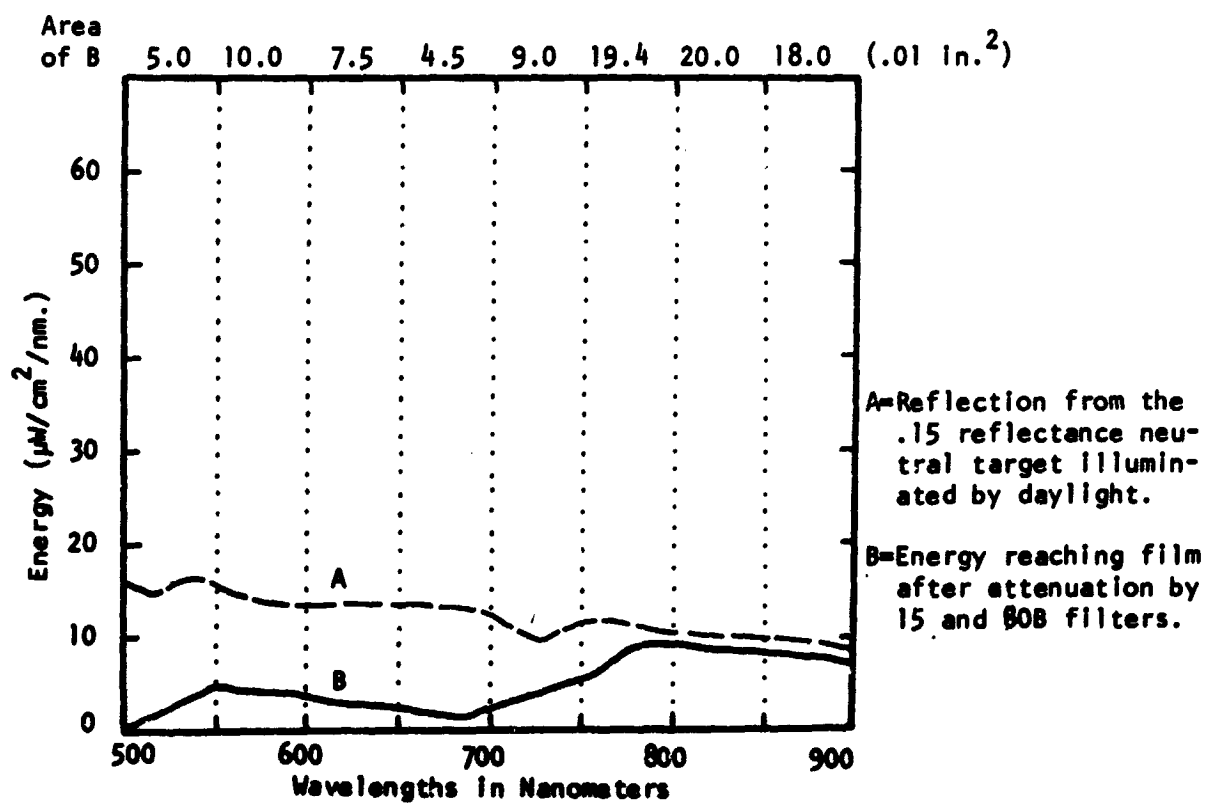
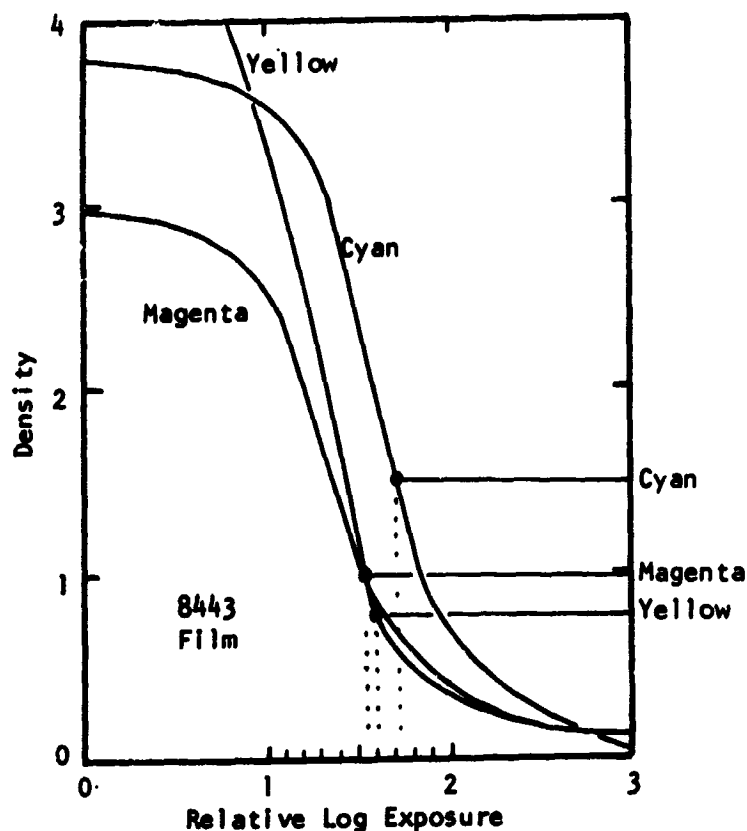


Figure 11. Reflection from a neutral target reshaped by an 80B auxiliary filter. Note that dye-layer densities are close with only a slight blue (cyan and magenta) predominance.

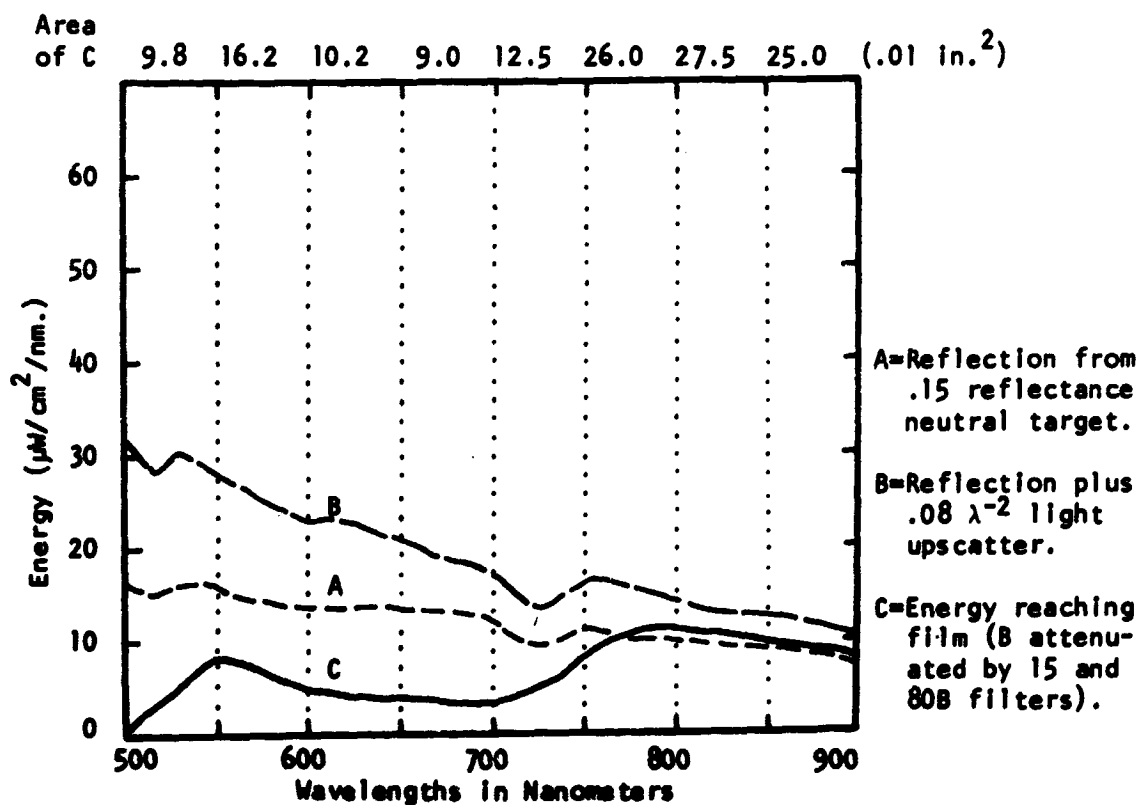


A=Reflection from the .15 reflectance neutral target illuminated by daylight.

B=Energy reaching film after attenuation by 15 and 80B filters.



**Figure 12. Reflection from the neutral target illuminated by daylight with air luminance added. Note that the cyan again becomes prominent despite the use of an 80B auxiliary filter.**





Soil and weathered rock surfaces are important components of non-urban images. For these, a reflectance that rises steadily from the visual into the infrared appears to be typical. Although this built-in IR exposure advantage is insufficient to prevent a cyan dominance when only a 15 filter is used, 80B attenuation lowers the cyan density to approximately that of the other layers and neutral tones ensue. An 80B rather drastically attenuates the energy in the visual wavelengths. It can thus maintain close to neutral soil tones even at high altitudes as is illustrated by Figure 13. Minus-visual filters, which attenuate the visual wavelengths less than the 80B, do not yield neutral tones at high altitude from soil targets. This is illustrated by Figure 14 where a CC30B is used at the camera in conjunction with a 15. Cyan and yellow predominate. The result is a true green for many soil targets when this auxiliary is used.

#### SUMMARY

The foregoing describes a method whereby the relative dye-layer densities of Type 8443 color infrared transparency film can be predicted without the aid of elaborate computing devices. In so doing it quantitatively substantiates existing experience with the use of minus-visual filters for combating the effects of high altitude. An obvious next step is the transformation of the relative dye-layer densities into actual color hues and tones.

Although there is no attempt here to provide a precise method for this color synthesis, subjective evaluations can be made. First, it is necessary for the cyan density to be lower than those of the other two layers for a red record to show. Since the cyan, or the lack of it, only provides the window through which the red color shows, it is necessary that the magenta and yellow have sufficient density to yield in concert the desired red.

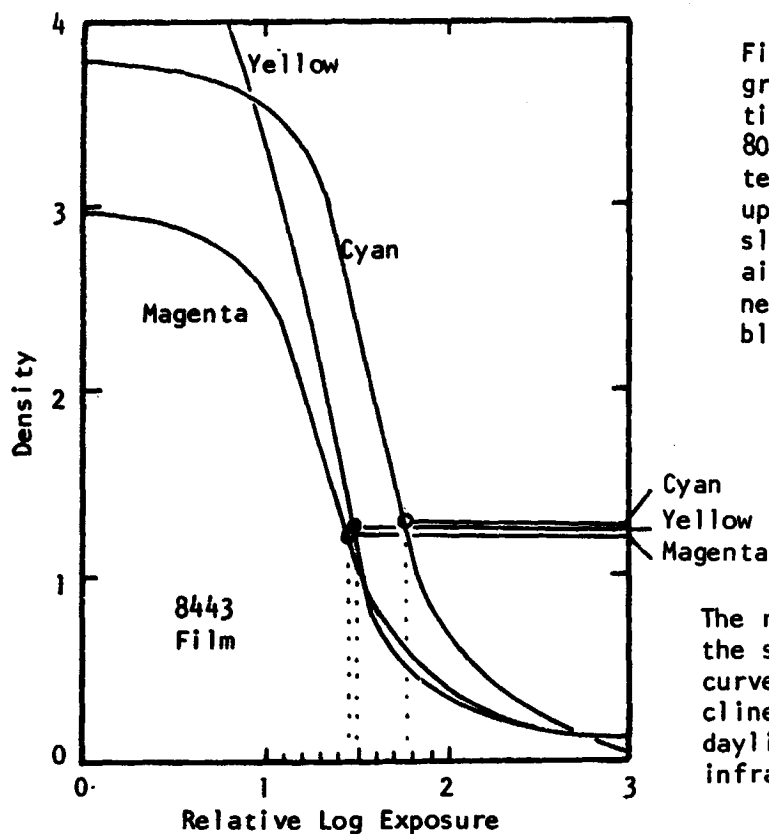
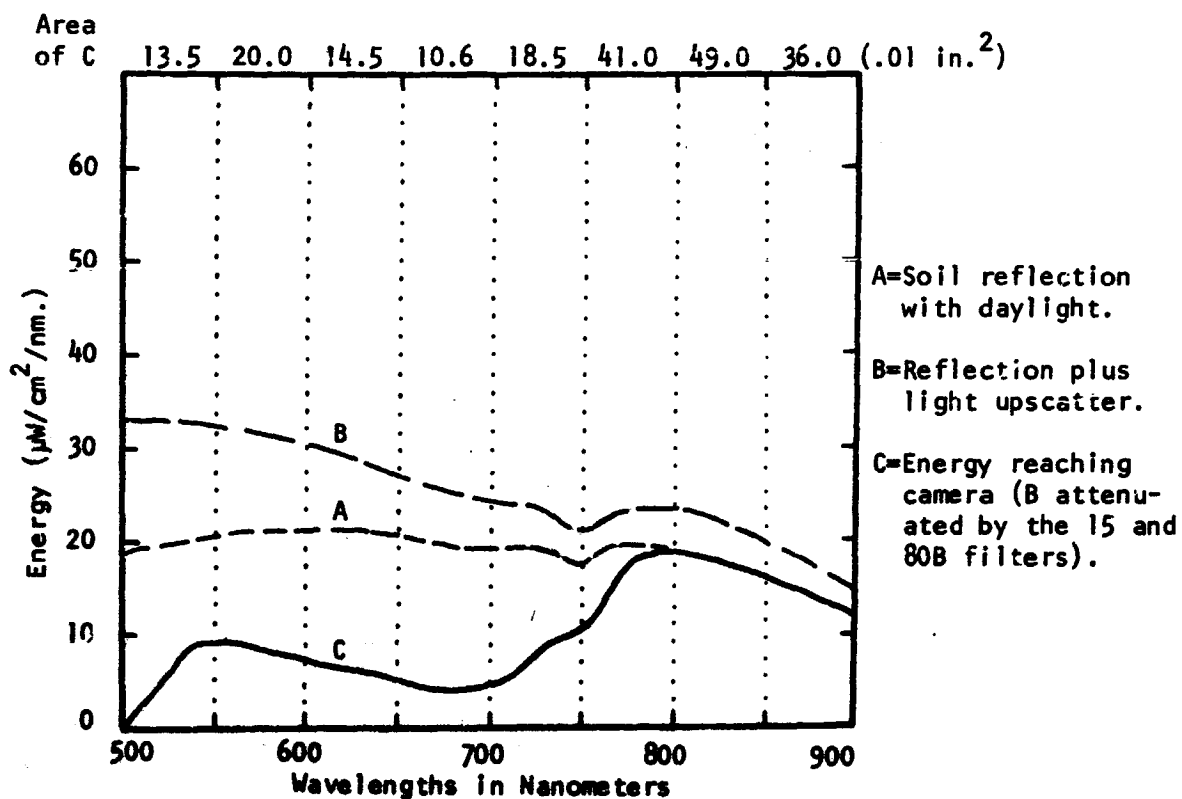


Figure 13. Weathered granitic soil reflection aloft using an 80B with the 15 filter. With a  $.08 \lambda^{-2}$  upscatter the soil is slightly red. More air luminance makes it neutral or slightly blue.

The rising IR reflectance of the soil does not show in curve A below due to the decline in intensity of the daylight spectrum at the infrared end.



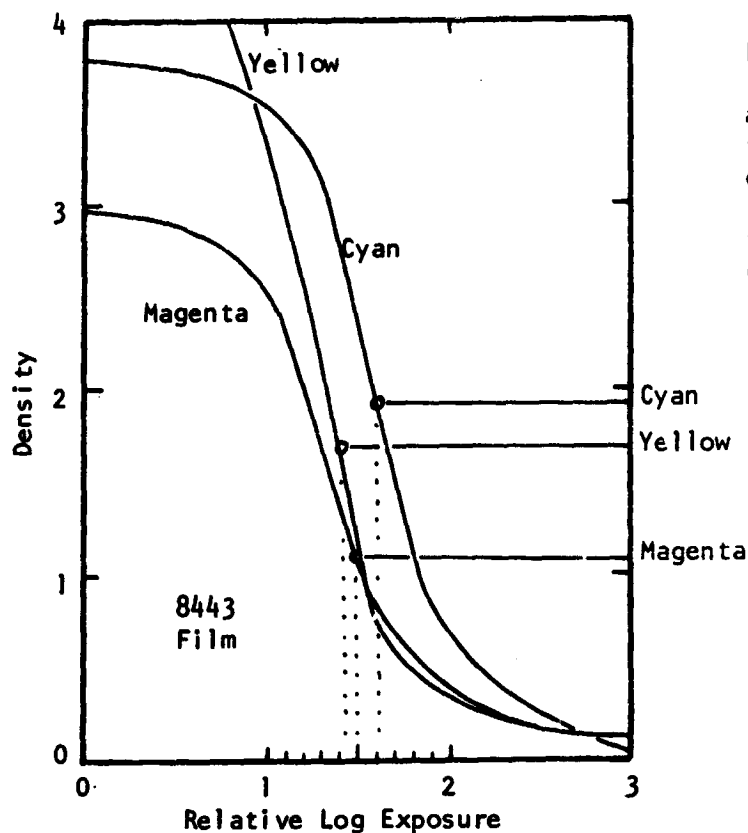
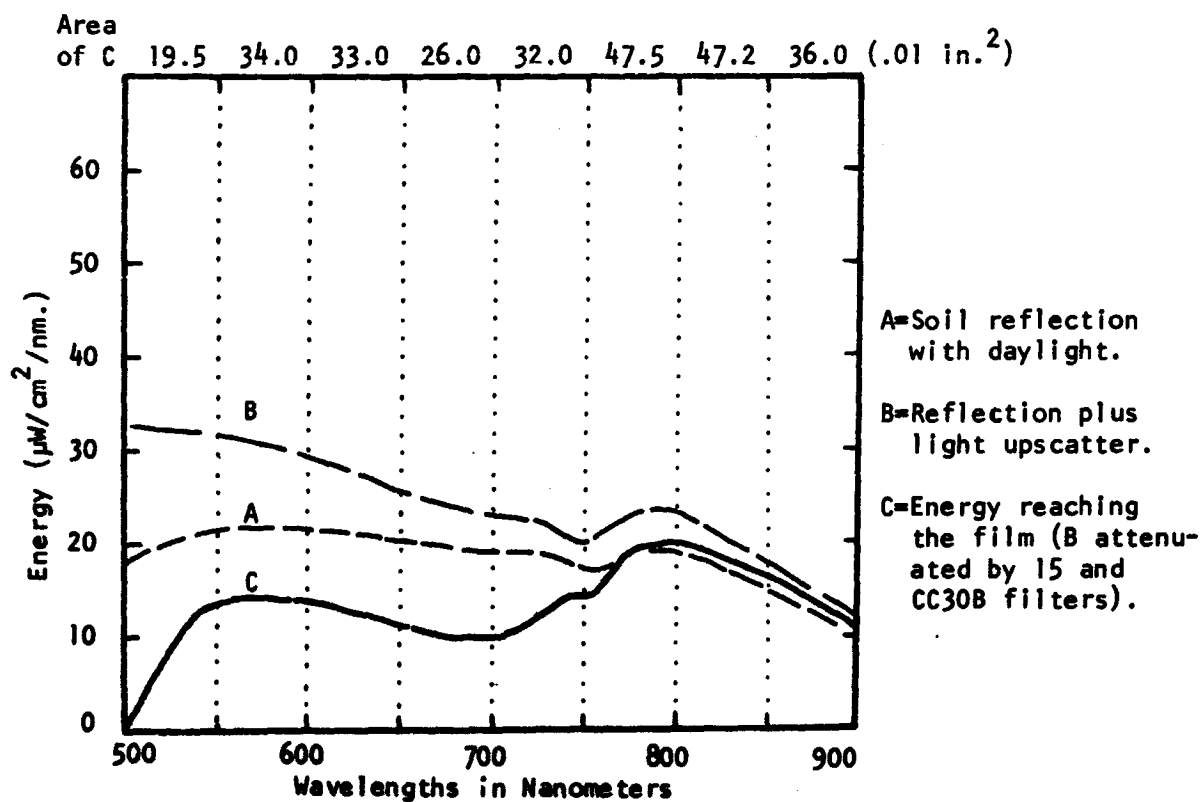


Figure 14. Granitic soil reflection aloft using a CC30B in addition to the 15 filter. Reshaping of the visual portion of the energy curve is less than with the 80B and cyan is dominant.



Second, the lowest density will set the neutral density or tone level of the color. If this is high, the overall tone will be dark. If this is low, the overall tone may be light. The departure of the other two densities from that of the lowest density can be considered as setting the color hue. If the neutral level is low, but the other densities are high, bright colors will result. If conversely, the neutral level is high and departure from that is only slight, dark unsaturated colors will result.

The two denser layers will set the color hue in proportion to their departures from the neutral density level. Should they be equally dense, the hue will divide between them, more frequently one dominates and the combination will favor the densest. These guidelines can be helpful in evaluating hue.

cyan + magenta → blue to purple

magenta + yellow → red

cyan + yellow → green

There are color systems whereby the tone and hue can be pinpointed with greater accuracy. The Munsell system is one. It is intriguing to consider the possibility that the process can be reversed and that a reflectance curve could be selected that would produce the dye-layer densities of an image target when the photographic parameters are known.

## BIBLIOGRAPHY

Brock, G.C., et al, 1965, Photographic Considerations for Aerospace. Itek Corporation, Lexington, Mass. 122 pp.

Fritz, Norman L., 1967, "Optimum Methods for Using Infrared-Sensitive Color Film," Photogrammetric Engineering, Vol. XXXIII, Number 10, (October) pp. 1128-1138.

Pease, R.W. and Bowden, L.W., 1968 "Making Color Infrared Film a More Effective High Altitude Remote Sensor," Remote Sensing: an Interdisciplinary Journal, Vol. 1 (in press).

Also issued as: Technical Letter NASA-117, May 1968, Manned Spacecraft Center, Houston, Texas.

Tarkington, R. and Sorem, A., 1963, "Color and False Color Films for Aerial Photography," Photogrammetric Engineering, Vol. XXIX, Number 1 (January) pp. 88-95.

## ADDENDUM

--

## COLOR INFRARED PHOTOGRAPHY THROUGH SPACECRAFT WINDOWS

All glass becomes opaque to long wavelengths of radiant energy. For most, significant decline in transmittance occurs at wavelengths far longer than those within the CIR spectrum. Spacecraft windows or ports, however, may have heat-shielding coatings which interfere with the transmission of the infrared energy that exposes the cyan-forming layer of color infrared film.

Two transmittance curves for spacecraft ports are shown in Figure 15. Curve A is described as being at an angle of incidence of  $45^{\circ}$  to the window and thus is assumed to be an off-axis condition. There is no stipulation for the angle through which measurements were made for curve B, purportedly the same window. Curve A represents deterioration from use in space.

In predicting the densities of CIR dye-layers of photographs taken through them, the windows are simply considered as additional attenuating filters. The ground target is the previously used pine needles to the reflection of which is added  $.08 \lambda^{-2}$  air luminance.

For curve A the transmittance drops so rapidly above 700 nm. that much of the exposure of the cyan-forming layer is lost. The use of minus-visual auxiliaries does not help since their rise in transmittance almost exactly is cancelled by the increasing opacity of the window. For the plotting in Figure 16 a 78B filter was used to attenuate the visual wavelengths since its peak density occurs at a somewhat shorter wavelength (650 nm.) than the 80B (700 nm.). Despite this precaution there is insufficient exposure of cyan layer to give a density lower than that of the other layers. No red

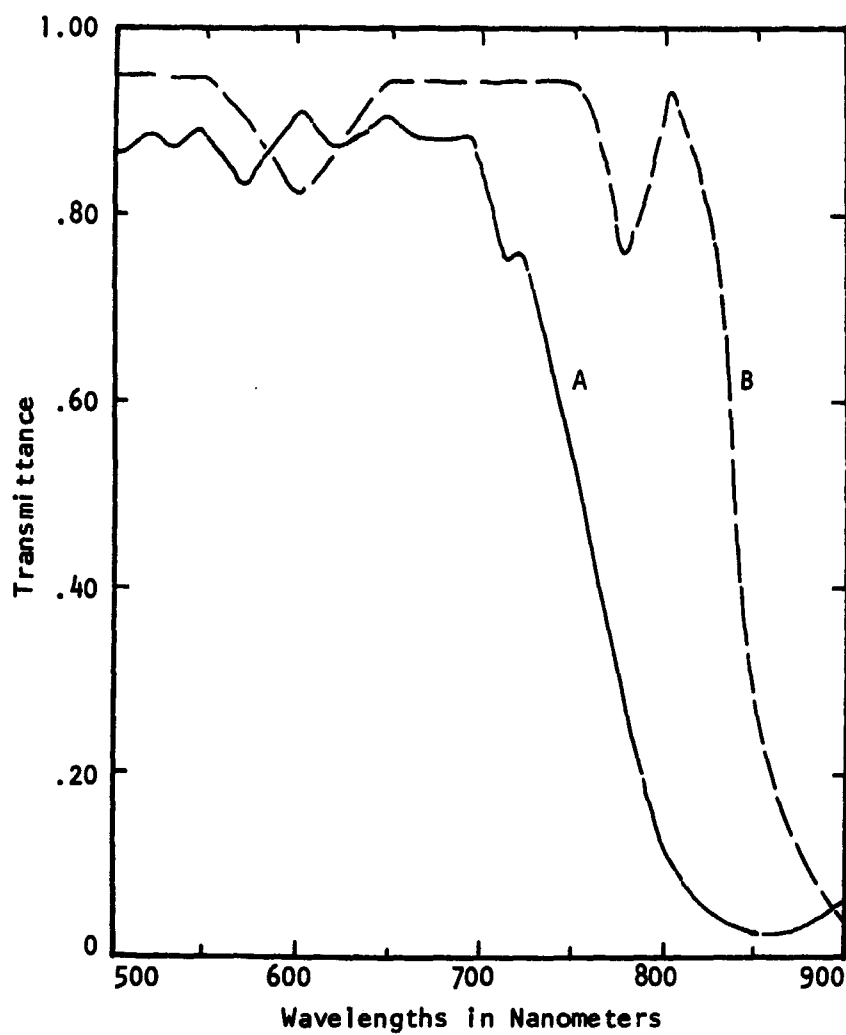


Figure 15. Transmittances of certain spacecraft windows or ports. Curve A, furnished by North American, is described as "45° Incidence." It is also noted as having deteriorated from use in space. Curve B, supplied by MSC is for the window transmittance before space use.

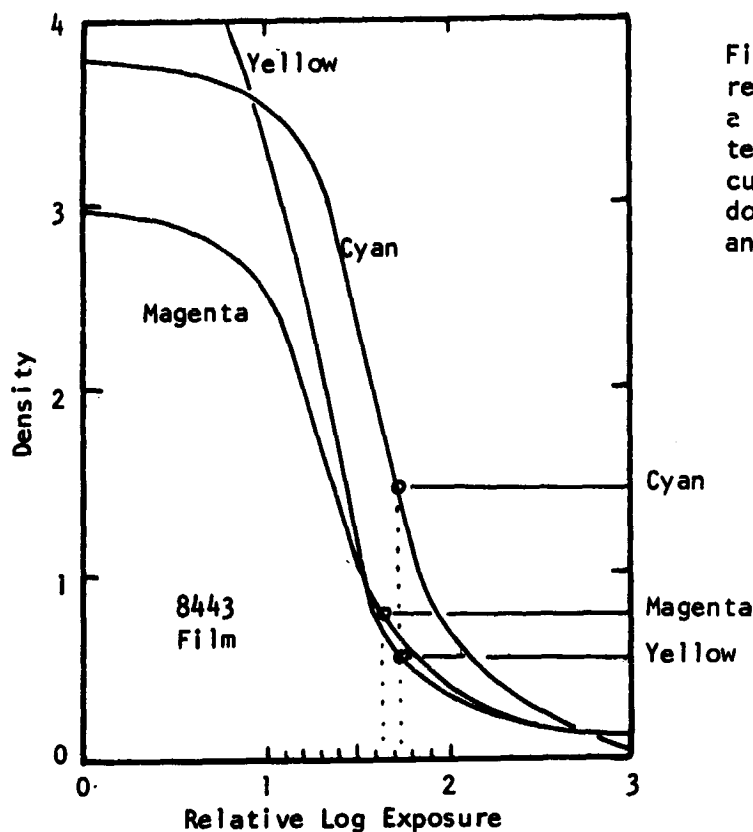
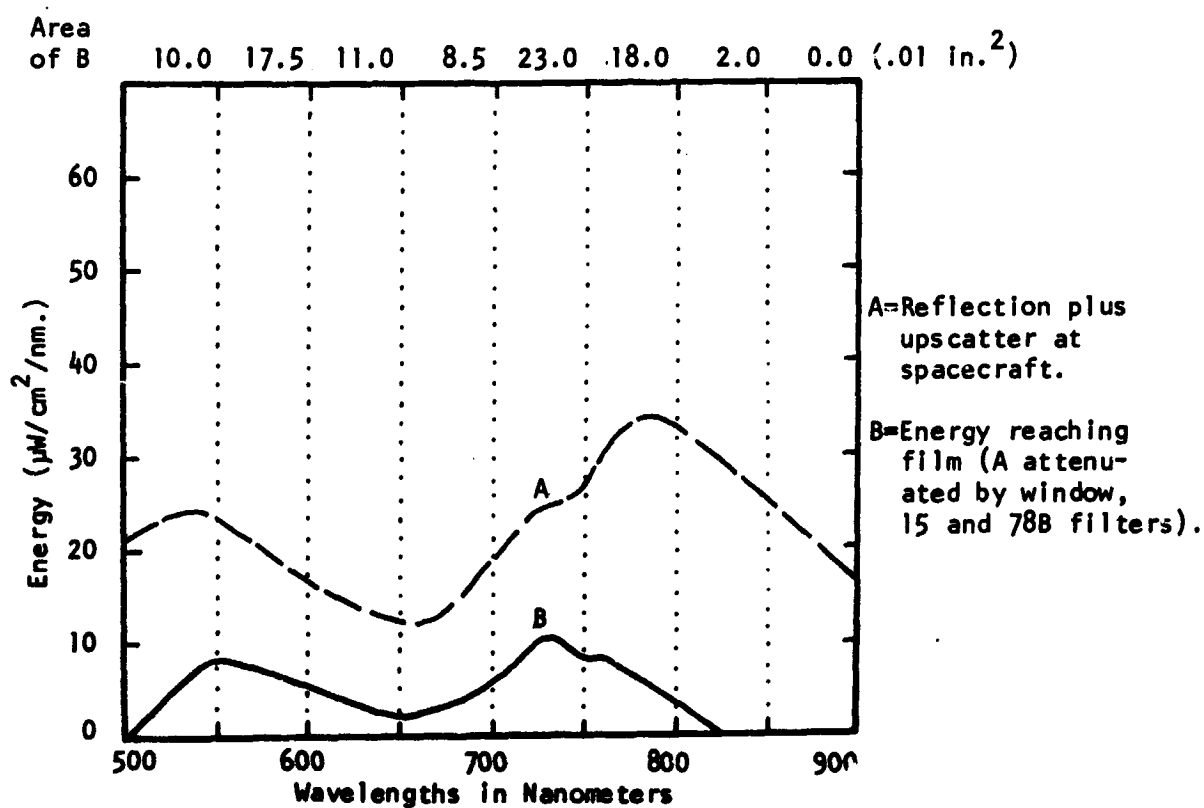


Figure 16. Pine needle reflection aloft plus  $\approx .08 \lambda^{-2}$  light upscatter, attenuated by a curve A spacecraft window in addition to 15 and 78B filters.





record could result from this target, although a high IR reflectance target such as grass might yield a purplish red color.

The transmittance of port B will yield a red record of the pine needle target with a 15 as the minus-blue filter to increase yellow and a 78B as the minus-visual auxiliary. This is demonstrated in Figure 17 where the cyan density is substantially lower than that of the other layers. Enough infrared exposure is available through this window that an 80B should also be a successful auxiliary, yielding only a slightly less red result than the 78B.

Pine needles have a relatively low IR/Visual reflectance ratio. Other targets such as grass in its vegetative stage, broadleaf forest, or most leafy crop plants would yield a brighter red. It can thus be concluded that with moderately clear conditions, color infrared photography through a port with a curve B transmittance would be quite successful, provided an appropriate minus-visual auxiliary filter such as the 78B or the 80B is used to combat the effects of high altitude.

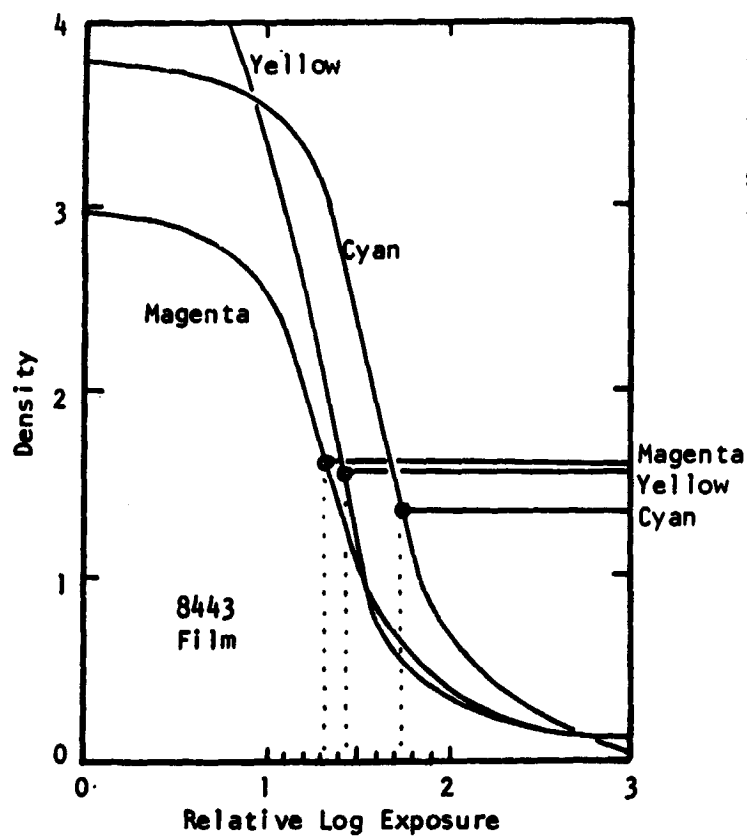
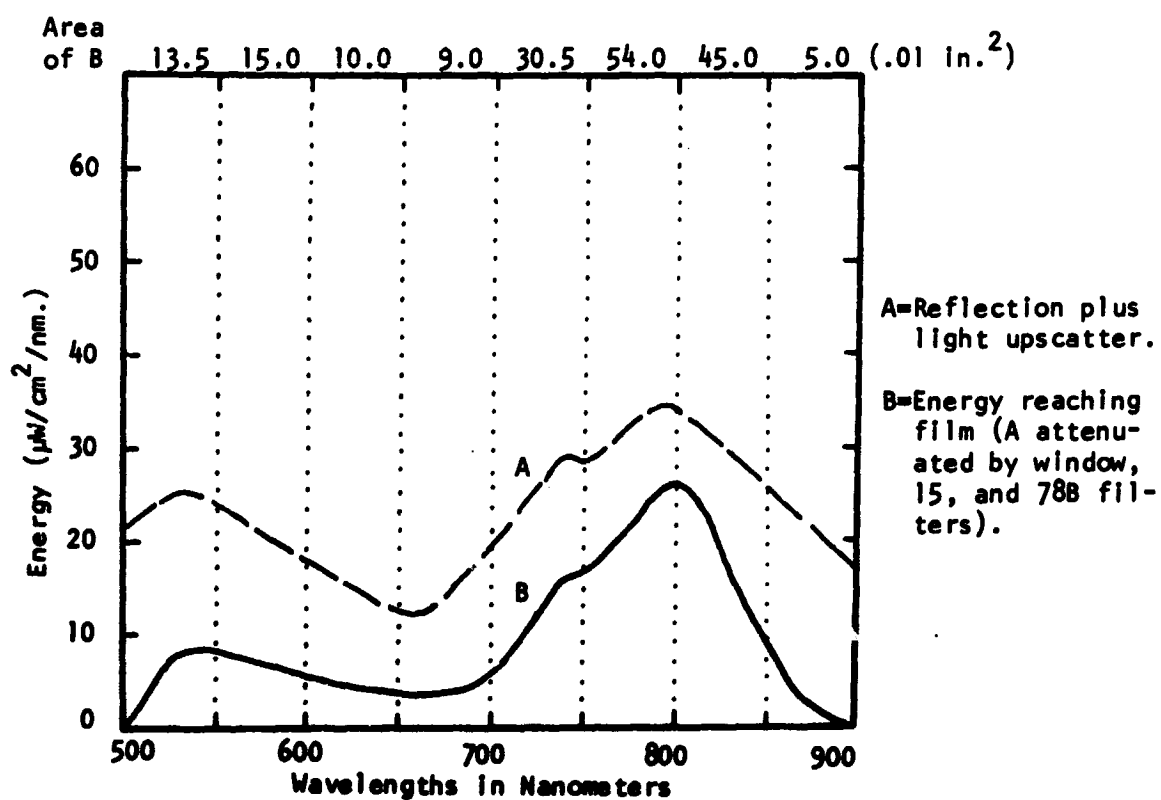


Figure 17. Pine needle reflection aloft plus an  $.08 \lambda^{-2}$  upscatter, attenuated by a curve B spacecraft window, 15, and 78B filters.

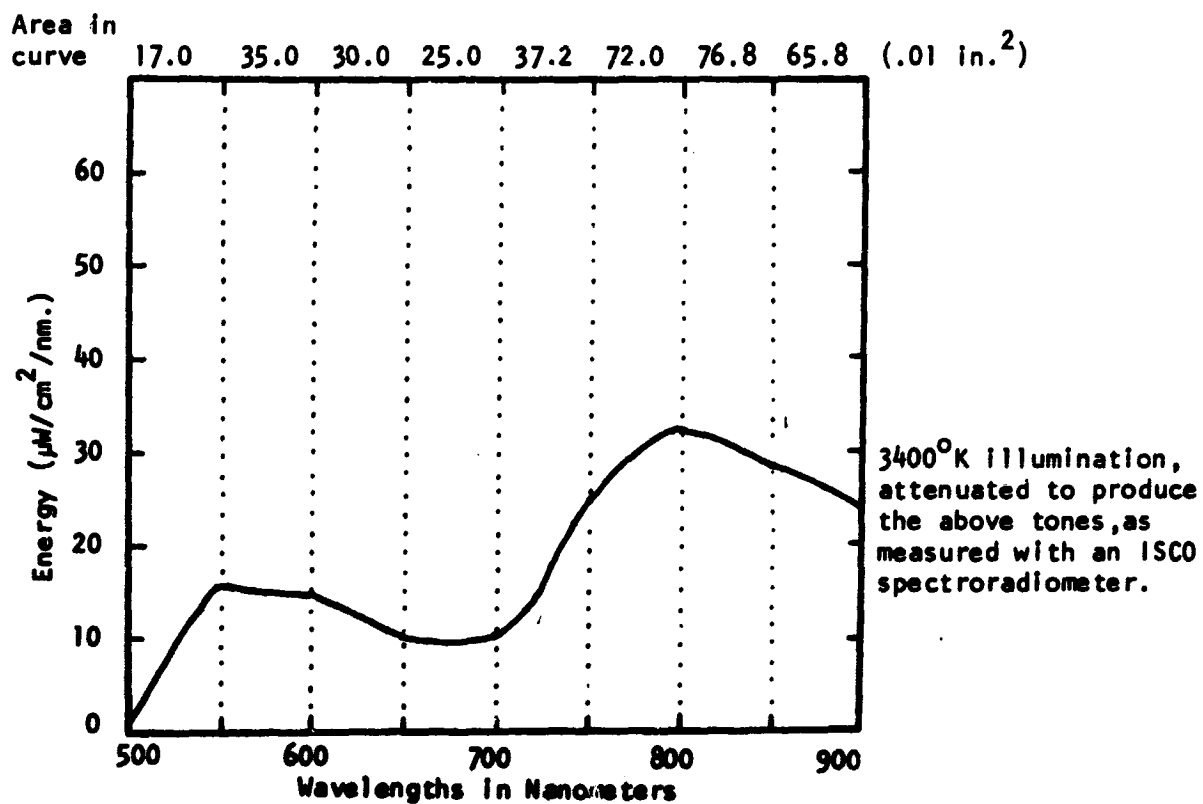
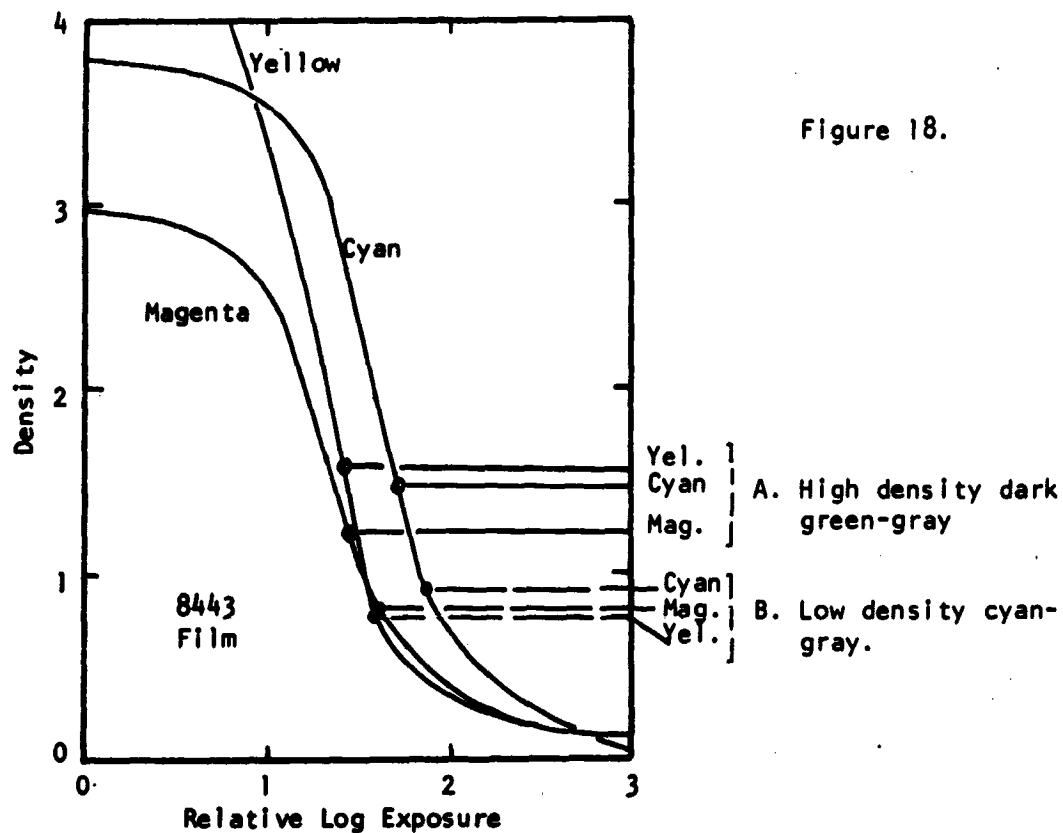


## APPENDIX

Modification of the D log E Diagram

A neutral target was photographed with 3400°K illumination and with filters that rendered CIR images, if not neutral, with low color saturation. The spectral distribution of the illumination, attenuated by all filters used and measured with an ISCO spectroradiometer, is shown at the bottom of Figure 18. The low exposure-high density result was a dark green-gray and is represented by A on the D log E diagram of Figure 18. The curves were adjusted so that cyan and yellow would equally predominate to represent this color. The long exposure-low density image was cyan-gray (B on D log E diagram). The curves were adjusted for this color so that yellow and magenta together would form the neutral color level with cyan alone predominating. The resulting sensitometric curves follow closely those of Fritz (1967) but are slightly modified to fit this method of dye-layer density analysis.

The following was used as a check of curve placement. It had been noted that a neutral target photographed through 15 and 78A filters with a low sun illumination produced close to perfectly neutral tones at moderate densities. Images with various densities were made under these conditions and the illumination, attenuated by the filters used, was measured with the spectroradiometer. The illumination curve is the lower graph of Figure 19. When plotted on the D log E diagram by the graphical method described, densities of the three dye-layers were virtually the same in each of two exposure examples.



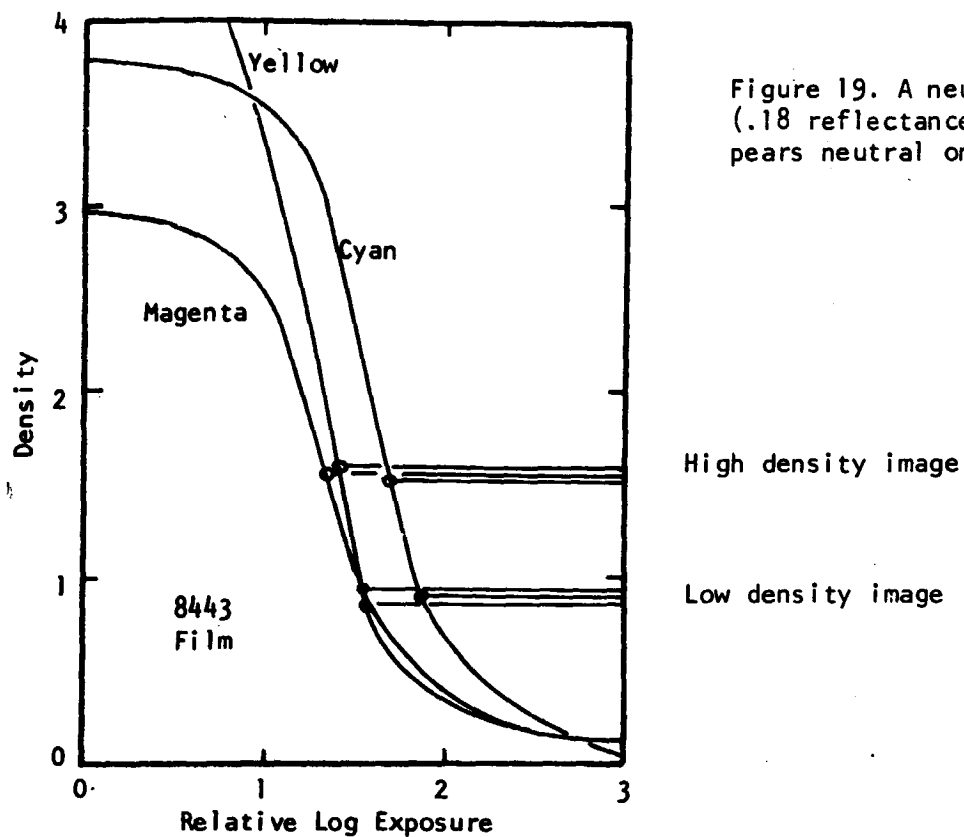
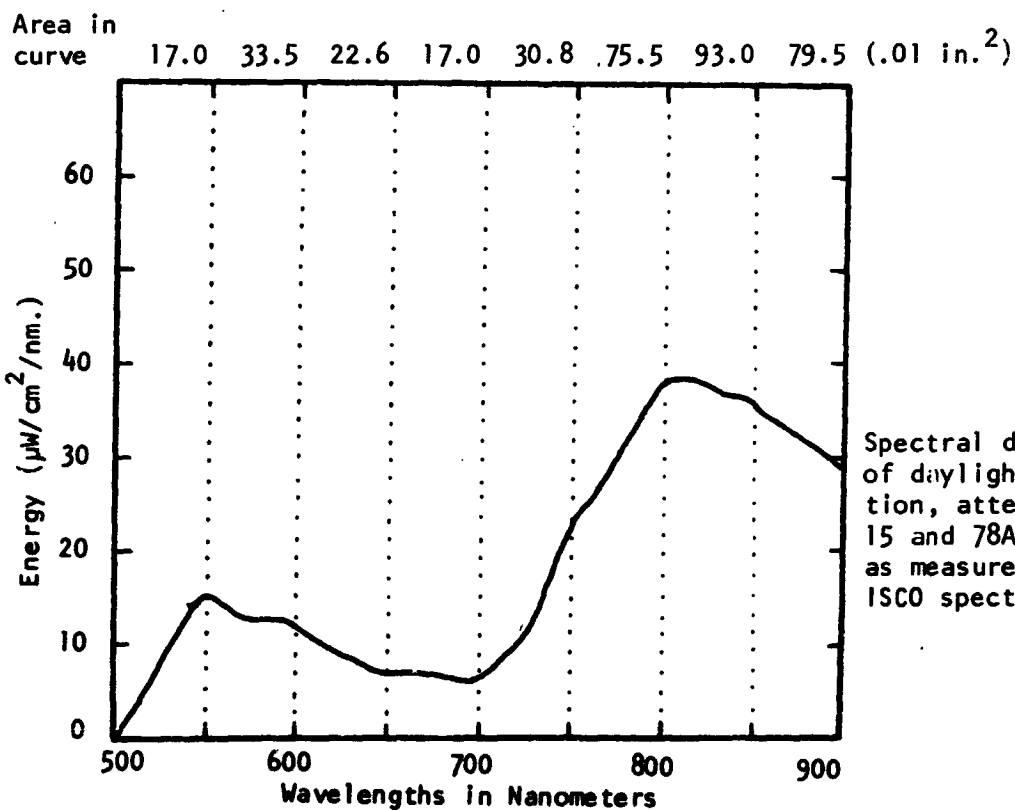


Figure 19. A neutral target (.18 reflectance) that appears neutral on a CIR image.



Spectral distribution of daylight illumination, attenuated by 15 and 78A filters, as measured with an ISCO spectroradiometer.